Materials International
Open Access Journal (ISSN: 2668-5728)

Review
Volume 7, Issue 2, 2025, 19
https://doi.org/10.33263/Materials72.019

On Topological Indices and Entropy Measures of Titanium Dioxide TiO_2 via Logarithmic Regression Model

Shilpa Haraloor Channakrishnappa [1,*], Gayathri Kamanna [1], Ballenahalli Ningegowda Dharmendra [2], Nagesh Hadonahalli Mudalagiraiah [3], Muhammad Kamran Siddiqui [4]

1 Department of Mathematics, School of Applied Sciences, REVA University, Kattigenahalli, Karnataka State, India; shilpahc539@gmail.com (S.H.C); gayathri.k@reva.edu.in (G.K.);
2 Department of Mathematics, Government College for Women, Kolar, India; bndharma@gmail.com;
3 Department of Science and Humanities, PES University, Bangalore, Karnataka State, India; nageshhm@pes.edu;
4 Department of Mathematics, COMSATS University Islamabad, Lahore Campus, Lahore, Pakistan; kamransiddiqui75@gmail.com;
* Correspondence: shilpahc539@gmail.com (S.H.C);

Received: 20.08.2024; Accepted: 2.01.2025; Published: 10.06.2025

Abstract: Titanium dioxide (TiO_2) is a nanomaterial widely used in various applications, including cosmetics and food additives. Due to its prevalent presence in everyday products, especially in nanoscale form, safety concerns have been raised. Topological indices, which mathematically represent molecular structures, and Shannon entropy, a measure of information content, have become powerful tools for analyzing the structural characteristics of these nanomaterials. In this study, we calculate the Nirmala index, along with the first and second inverse Nirmala indices, for titanium dioxide (TiO2) using its M-polynomial. The comparison of these indices and their corresponding entropy measures is demonstrated using numerical computation and 2D line plots. Also, a logarithmic regression model is constructed to explore the relationship between the Nirmala indices and their corresponding entropy measures. These findings may provide valuable insights for future advancements in the use of titanium dioxide (TiO_2) as a food additive or sunscreen compound.

Keywords: Nirmala index; first inverse Nirmala index; second inverse Nirmala index; graph entropy; titanium dioxide TiO_2.

1. Introduction

Titanium dioxide (TiO_2), also known as titania or titanium (IV) oxide, is a versatile material with a wide range of real-world and prospective uses. Known by many as “titanium white”, this fine white powder is mainly employed as a pigment due to its strength, opacifying ability, and hiding power. TiO_2 has a high refractive index, which allows it to scatter and absorb UV light and be chemically and thermally stable. Because of these qualities, titanium dioxide is a necessary component in the production of plastics, paints, and surface coatings. Three different crystal polymorphs of titanium dioxide exist: rutile, brookite, and anatase.

Since both rutile and anatase change into rutile at temperatures above 800°C, rutile is the most thermally stable. Due to differences in their band gaps within the TiO_2 electron structures, the photoactive characteristics of TiO_2 are present in all of its crystal forms. The global production of titanium dioxide worldwide is continuously rising [1]. Titanium dioxide is widely used as an additive in paints, plastics, personal care products (such as cosmetics and sunscreens), and food (as the additive E171) [2,3]. Due to their significantly reduced particle size, which imparts unique properties compared to macro or microparticles, titanium(IV) oxide nanoparticles have garnered considerable interest from research groups [4]. In the medical sciences, TiO_2 has been investigated as an effective drug carrier (e.g., TiO2 nanotubes) [5] and for skin tissue engineering and wound dressings [6-8]. Nanoscale TiO_2 particles also exhibit notable photocatalytic properties, including the ability to mediate the photodegradation of pharmaceuticals, inactivate bacteria, exert a photooxidative killing effect on cancer cells, and assist in energy storage, as well as air and water purification [9]. Today, TiO_2 nanoparticles are among the most widely produced nanomaterials globally [10].

Recently, the European Food Safety Authority (EFSA) raised concerns about the safety of titanium dioxide (E171) in food products containing nano- and microparticles, citing potential genotoxicity. However, opinions on its safety remain divided. To address these concerns, a thorough assessment of titanium dioxide's genotoxic potential was conducted based on a comprehensive review of 192 datasets covering relevant endpoints and test systems. Only 34 datasets were deemed reliable and of high quality for evaluating genotoxicity. Among these, 10 datasets reported positive findings, indicating genotoxic effects such as DNA strand breakage and chromosome damage. Notably, these effects were associated with conditions of high cytotoxicity, oxidative stress, inflammation, apoptosis, necrosis, or their combinations. The assessment suggests that the observed genotoxic effects of titanium dioxide, including nanoparticles, are likely secondary to physiological stress rather than direct mutagenicity. Importantly, the in vitro and in vivo gene mutation studies that were looked at did not yield any positive results. However, stronger studies would be needed to reach a firm conclusion on mutagenicity [11]. The various applications of titanium dioxide nanoparticles are discussed in [12,13].

1.1. Literature review for titanium dioxide.

The network construction and module detection for the molecular graph of titanium dioxide are studied in [13]. Latha *et al*. [14] and Zhu *et al*. [15] showed that titanium dioxide nanotubes can stop HMGB1. This cytokine plays a role in how cells respond to infection, injury, and inflammation. TiO_2 nanoparticles cause brain damage and oxidative stress, a difference between free radicals and antioxidants in humans [16,17]. It also initiated apoptosis, a group of distinct protease pathways that kill cells in specific ways [18,19]. Even in very small amounts, these particles had these effects [20,21]. The oxide titanium dioxide is stable chemically and is safe for the environment. It comes in different crystal forms, including rutile, brookite, anatase, baddeleyite, columbite, TiO_2(B), ramsdellite, hollandite-like, TiO_2-OI, TiO_2-OII, and fluorite, such as the cubic phase [22,23]. Of these stages, rutile, brookite, and anatase are all found in nature. Brookite and anatase are less stable than rutile. Brookite and anatase are metastable and change into rutile when heated [24]. The lattice values for rutile are a = 0.459 nm, b = 0.459 nm, and c = 0.296 nm. It has a tetragonal crystal structure [25]. The entropy value for rutile is 50.35 JK^{-1} mol^{-1}, and the enthalpy for rutile is 8.635 $KJmol^{-1}$ [26].

In this article, we calculate the Nirmala index and the first and second inverse Nirmala indices for titanium dioxide (TiO_2) using its M-polynomial. The corresponding entropy measures are found using Shannon's method. Also, a logarithmic regression model is constructed to explore the relationship between the Nirmala indices and their corresponding entropy measures.

1.2. Chemical graph theory and discussion of the topic.

A numerical parameter, a topological index, is used to represent a compound's molecular structure by analyzing its graph-theoretical properties. In the context of quantitative structure-activity relationship (QSAR) and quantitative structure-property relationship (QSPR) studies, topological indices serve as predictive tools for the physicochemical properties of chemical compounds. Graph entropies have evolved into information-theoretic instruments for exploring the structural information of molecular graphs.

Let $V(G)$ and $E(G)$ denote the vertex set and edge set of the molecular graph G, respectively. The total number of edges incident to a vertex $v \in V(G)$ is its $degree$, denoted by $d_G(v)$. For an edge $e = uv$ of the graph G, u, and v are the end vertices of the edge e. The topological index [27] based on degrees of a graph G given its edge set $E(G)$ is given by

$$I(G) = \sum_{uv\in E(G)} \chi\left(d_G(u), d_G(v)\right) \qquad (1)$$

$\chi(x, y)$ is a non-negative and symmetric function that depends on the mathematical formulation of the topological index.

As studied in the literature, many topological indices have shown benefits in many fields, including computer science, physics, biology, chemistry, and drug development. The first and most studied topological index, the Wiener index, was developed by H. Wiener in 1947. One important application for it [28] is paraffin boiling temperature projection. Another well-known degree-based topological statistic was developed by Milan Randić in 1975 and is sometimes called the Randić index. Its importance in the development of drugs is studied [29]. To improve the prediction ability of degree-based topological indices, several attempts have been made to supplement them with new indices.

A unique degree-based topological index of a molecular graph G, known as the Nirmala index $N(G)$, was recently introduced by Kulli [30].

$$N(G) = \sum_{uv\in E(G)} \sqrt{d_G(u) + d_G(v)} \quad (2)$$

In 2021, Kulli [31] defined the first inverse Nirmala index $IN_1(G)$ and second inverse Nirmala index $IN_2(G)$ of a molecular graph G.

$$IN_1(G) = \sum_{uv\in E(G)} \sqrt{\frac{1}{d_G(u)} + \frac{1}{d_G(v)}} = \sum_{uv\in E(G)} \left(\frac{1}{d_G(u)} + \frac{1}{d_G(v)}\right)^{\frac{1}{2}} \qquad (3)$$

$$IN_2(G) = \sum_{uv\in E(G)} \frac{1}{\sqrt{\frac{1}{d_G(u)} + \frac{1}{d_G(v)}}} = \sum_{uv\in E(G)} \left(\frac{1}{d_G(u)} + \frac{1}{d_G(v)}\right)^{-\frac{1}{2}} \qquad (4)$$

Previously, the standard mathematical definition of multiple topological indices was used to calculate topological indices. Many efforts have been made to discover a short way to recover many topological indices for a given class. In this context, the notion of a general polynomial was established, whose derivatives, integrals, or a combination of both can be used to determine the values of the required topological indices at a given point. For instance, neighborhood-degree-sum-based topological indices are obtained from the NM polynomial [32], whereas distance-based topological indices are obtained from the Hosoya polynomial [33]. Deutsch and Klažar [34] presented the M-polynomial in 2015 as a method for determining the degree-based topological index.

Definition 1.1 ([34]) The M-polynomial of a graph G is defined as $(G; x, y) = \sum_{\delta\le i\le j\le\Delta} m_{i,j}(G)x^i y^j$,

where $\delta = min\{d_G(u)|u \in V(G)\}, \Delta = max\{d_G(u)|u \in V(G)\}$ and m_{ij} is the number of edges $uv \in E(G)$ such that $d_G(u) = i, d_G(v) = j\ (i, j \ge 1)$.

The M-polynomial-based derivation formulas to compute the different Nirmala indices are listed in Table 1.

Table 1. Relationship between the M-polynomial and Nirmala indices for a graph G.

Sl. No	Topological Index	$\chi(x,y)$	Derivation from $M(G;x,y)$
1	Nirmala index (N)	$\sqrt{x+y}$	$D_x^{\frac{1}{2}}J(M(G;x,y))\|_{x=1}$
2	First inverse Nirmala index (IN_1)	$\sqrt{\left(\frac{x+y}{xy}\right)}$	$D_x^{\frac{1}{2}}JS_y^{\frac{1}{2}}S_x^{\frac{1}{2}}(M(G;x,y))\|_{x=1}$
3	The second inverse Nirmala index (IN_2)	$\sqrt{\left(\frac{xy}{x+y}\right)}$	$S_x^{\frac{1}{2}}JD_y^{\frac{1}{2}}D_x^{\frac{1}{2}}(M(G;x,y))\|_{x=1}$

Here, $D_x^{\frac{1}{2}}(h(x,y)) = \sqrt{x \cdot \frac{\partial(h(x,y))}{\partial x}} \cdot \sqrt{h(x,y)}$; $D_y^{\frac{1}{2}}(h(x,y)) = \sqrt{y \cdot \frac{\partial(h(x,y))}{\partial y}} \cdot \sqrt{h(x,y)}$; $S_x^{\frac{1}{2}}(h(x,y)) = \sqrt{\int_0^x \frac{h(t,y)}{t} dt} \cdot \sqrt{h(x,y)}$; $S_y^{\frac{1}{2}}(h(x,y)) = \sqrt{\int_0^y \frac{h(x,t)}{t} dt} \cdot \sqrt{h(x,y)}$;

And $J(h(x,y)) = h(x,x)$ are the operators.

Shannon [35] introduced the fundamental concept of entropy in 1948, defining it as a measurement of the uncertainty of the information contained in a system, represented by a probability distribution. Later, entropy was used to assess the structural information of networks, graphs, and chemical structures. In the past few years, graph entropies have gained increased utility in several fields, including mathematics, computer science, biology, chemistry, sociology, and ecology. There are various forms of graph entropy measurements, including extrinsic and intrinsic measures. These measures relate to the probability distribution concerning graph invariants, such as edges and vertices. Readers are referred to [36-38] for additional details on degree-based graph entropy measures and their applications.

1.3. Entropy of a graph in terms of vertex degree.

Let G be a simple and connected graph of order p and size q. Then, the graph entropy of G [35] is defined as follows:

$$ENT_{\omega}(G) = -\sum_{i=1}^{p} \frac{\omega(s_i)}{\sum_{j=1}^{p}\omega(s_j)} log\left(\frac{\omega(s_i)}{\sum_{j=1}^{p}\omega(s_j)}\right) \qquad (5)$$

Here, ω is a meaningful information function and $s_i \in V(G)$ for every $i \in [1,2,\dots,p]$.

Let $\omega(s_i) = d_{\Upsilon}(s_i)$. Then equation (5) reduces to:

$$ENT_{\omega}(G) = -\sum_{i=1}^{p} \frac{d_G(s_i)}{\sum_{j=1}^{p} d_G(s_j)} log\left(\frac{d_G(s_i)}{\sum_{j=1}^{p} d_G(s_j)}\right)$$

$$= log\left(\sum_{j=1}^{p} d_G(s_j)\right) - \frac{1}{\sum_{j=1}^{p} d_G(s_j)} \sum_{i=1}^{p} d_G(s_i) log(d_G(s_i))$$

By the fundamental theorem of graph theory, $\sum_{i=1}^{p} d_G(s_i) = 2q$. Thus,

$$ENT_{\omega}(G) = log(2q) - \frac{1}{2q}\sum_{i=1}^{p} d_G(s_i) log(d_G(s_i)) \qquad (6)$$

1.4. Entropy of a graph in terms of edge-weight.

Chen *et al*. [39] proposed the concept of the entropy of edge-weighted graphs as follows: Consider the edge-weight graph $G = (V(G), E(G), \omega(st))$, in which $E(G)$ represents the set of edges, $V(G)$ represents the set of vertices, and $\omega(st)$ represents the weight of an edge $st \in E(G)$. Then, given an edge weight, the entropy of a graph is defined as follows:

$$ENT_\omega(G) = -\sum_{s't' \in E(G)} \frac{\omega(s't')}{\sum_{st \in E(G)} \omega(st)} log\left(\frac{\omega(s't')}{\sum_{st \in E(G)} \omega(st)}\right)$$

$$= -\sum_{s't' \in E(G)} \frac{\omega(s't')}{\sum_{st \in E(G)} \omega(st)} \left[log(\omega(s't')) - log\left(\sum_{st \in E(G)} \omega(st)\right)\right]$$

$$= log\left(\sum_{st \in E(G)} \omega(st)\right) - \sum_{s't' \in E(G)} \frac{\omega(s't')}{\sum_{st \in E(G)} \omega(st)} log(\omega(s't'))$$

Thus, $ENT_\omega(G) = log\left(\sum_{st \in E(G)} \omega(st)\right) - \frac{1}{\left(\sum_{st \in E(G)} \omega(st)\right)} \sum_{s't' \in E(G)} \omega(s't') log(\omega(s't'))$ (7)

Virendra Kumar *et al.* [40] introduced the concept of the Nirmala indices-based entropy. To study this, they examined the relevant information function ω as a function related to the equations (2-4) that define the Nirmala indices.

Nirmala entropy: Let $\omega(st) = \sqrt{d_G(s) + d_G(t)}$. Then, from the definition of the Nirmala index as given in equation (2), we have

$\sum_{st \in E(G)} \omega(st) = \sum_{st \in E(G)} \sqrt{d_G(s) + d_G(t)} = N(G)$. Hence, using equation (7), the Nirmala entropy of a graph G is given by

$$ENT_N(G) = log(N(G)) - \frac{1}{N(G)} \sum_{st \in E(G)} \sqrt{d_G(s) + d_G(t)} \times log\left(\sqrt{d_G(s) + d_G(t)}\right) \quad (8)$$

First inverse Nirmala entropy: Let $\omega(st) = \sqrt{\frac{1}{d_G(s)} + \frac{1}{d_G(t)}}$. Then, from the definition of the first inverse Nirmala index as given in Equation (3), we have,

$$\sum_{st \in E(G)} \omega(st) = \sum_{st \in E(G)} \sqrt{\frac{1}{d_G(s)} + \frac{1}{d_G(t)}} = IN_1(G)$$

Hence, using equation (7), the first inverse Nirmala entropy of a graph G is given by

$$ENT_{IN_1}(G) = log(IN_1(G)) - \frac{1}{IN_1(G)} \sum_{st \in E(G)} \sqrt{\frac{1}{d_G(s)} + \frac{1}{d_G(t)}} \times log\left(\sqrt{\frac{1}{d_G(s)} + \frac{1}{d_G(t)}}\right) \quad (9)$$

Second inverse Nirmala entropy: Let $\omega(st) = \frac{\sqrt{d_G(s) \cdot d_G(t)}}{\sqrt{d_G(s) + d_G(t)}}$. Then, from the definition of the second inverse Nirmala index as given in Equation (4), we have,

$$\sum_{st \in E(G)} \omega(st) = \sum_{st \in E(G)} \frac{\sqrt{d_G(s) \cdot d_G(t)}}{\sqrt{d_G(s) + d_G(t)}} = IN_2(G)$$

Hence, using equation (7), the second inverse Nirmala entropy of a graph G is given by

$$ENT_{IN_2}(G) = log(IN_2(G)) - \frac{1}{IN_2(G)} \sum_{st \in E(G)} \frac{\sqrt{d_G(s) \cdot d_G(t)}}{\sqrt{d_G(s) + d_G(t)}} \times log\left(\frac{\sqrt{d_G(s) \cdot d_G(t)}}{\sqrt{d_G(s) + d_G(t)}}\right) \quad (10)$$

1.5. Motivation and research gap.

Extensive research has been carried out on the properties and applications of titanium dioxide nanoparticles. The review [12] compiles and analyzes the latest data on the safety of TiO_2 nanoparticles when used in food additives and sunscreen products. Currently, international authorities have not provided specific guidelines for the comprehensive assessment of TiO_2 nanoparticles in these products.

To address this gap, Nirmala-based topological indices of TiO_2 have been used by utilizing [13]. These findings could significantly influence the future use of titanium dioxide in food and sunscreen formulations.

2. Results and Discussion

In this section, we present generalized formulas for computing the Nirmala index and the first and second inverse Nirmala indices for TiO_2 using its M-polynomial. Further, we expand the process of finding information entropy measures using the Shannon method. When we refer to TiO_2, we mean $[\alpha \times \beta]$ cell of TiO_2, unless otherwise specified.

Let G be the molecular graph of the titanium dioxide TiO_2. Then the order and size of G are $4\alpha + 2\beta + 7\alpha\beta + 2$ and $12\alpha\beta + 2\alpha$, respectively. The vertex set and edge set partitions of G are given in Tables 2 and 3, respectively.

Table 2. Vertex set partition of G according to the degrees of each vertex.

Sl. No	Vertex set	$d_G(r)$	Number of repetitions
1	V_1	1	$2\beta + 6$
2	V_2	2	$8\alpha + 2\beta - 6$
3	V_3	3	$6\alpha\beta - 4\alpha - 2\beta + 2$
4	V_4	4	$\alpha\beta$

Table 3. Edge set partition of G according to the degrees of end vertices of an edge.

Sl. No	Edge set	$(d_G(r), d_G(s))$	Number of repetitions
1	E_1	(1,2)	4
2	E_2	(1,3)	$2\beta + 2$
3	E_3	(2,2)	$4\alpha - 4$
4	E_4	(2,3)	$4\alpha + 4\beta - 8$
5	E_5	(2,6)	4α
6	E_6	(3,3)	$6\alpha\beta - 6\alpha - 6\beta + 6$
7	E_7	(3,6)	$6\alpha\beta - 4\alpha$

2.1. Nirmala indices of titanium dioxide TiO_2

We now find the M-polynomial of TiO_2 as follows.

Theorem 1 Let G be the molecular graph of the titanium dioxide TiO_2. Then the M-polynomial of G is

$$M(G;x,y) = 4xy^2 + (2\beta + 2)xy^3 + (4\alpha - 4)x^2y^2 + (4\alpha + 4\beta - 8)x^2y^3 + 4\alpha x^2y^6 + (6\alpha\beta - 6\alpha - 6\beta + 6)x^3y^3 + (6\alpha\beta - 4\alpha)x^3y^6$$

Proof. The proof follows from Definition 1.1 and Table 3.

Now, we evaluate the Nirmala indices of TiO_2 with the help of its M-polynomial.

Theorem 2 Let G be the molecular graph of the titanium dioxide TiO_2. Then the Nirmala indices of G are:

a. $N(G) = (6\sqrt{6} + 18)\alpha\beta + \left(4\sqrt{5} + 4\sqrt{8} - 6\sqrt{6} - 4\right)\alpha + \left(4 + 4\sqrt{5} - 6\sqrt{6}\right)\beta + \left(4\sqrt{3} - 4 - 8\sqrt{5} + 6\sqrt{6}\right)$,

b. $IN_1(G) = (2\sqrt{6} + 3\sqrt{2})\alpha\beta + (4 + 4\sqrt{\frac{5}{6}} + 4\sqrt{\frac{2}{3}} - 2\sqrt{6} - 2\sqrt{2})\alpha + (\frac{4}{\sqrt{3}} + 4\sqrt{\frac{5}{6}} - 2\sqrt{6})\beta + 4\sqrt{6} + \frac{4}{\sqrt{3}} - 4 - 8\sqrt{\frac{5}{6}}$,

c. $IN_2(G) = (3\sqrt{6} + 6\sqrt{2})\alpha\beta + (4 + 4\sqrt{\frac{6}{5}} + 4\sqrt{\frac{3}{2}} - 3\sqrt{6} - 4\sqrt{2} - 3\sqrt{6})\alpha + (\sqrt{3} + 4\sqrt{\frac{6}{5}} - 3\sqrt{6})\beta + 4\sqrt{\frac{2}{3}} + \sqrt{3} - 4 - 8\sqrt{\frac{6}{5}} + 3\sqrt{6}$.

Proof. Let G be the molecular graph of the titanium dioxide TiO_2. From Theorem 1, the M-polynomial of G is given by

$M(G;x,y) = 4xy^2 + (2\beta+2)xy^3 + (4\alpha-4)x^2y^2 + (4\alpha+4\beta-8)x^2y^3 + 4\alpha x^2y^6 + (6\alpha\beta-6\alpha-6\beta+6)x^3y^3 + (6\alpha\beta-4\alpha)x^3y^6$. From Table 1, we have

i. $D_x^{\frac{1}{2}}J(M(G;x,y)) = D_x^{\frac{1}{2}}[4xy^2 + (2\beta+2)xy^3 + (4\alpha-4)x^2y^2 + (4\alpha+4\beta-8)x^2y^3 + 4\alpha x^2y^6]$

$$+D_x^{\frac{1}{2}}J[(6\alpha\beta-6\alpha-6\beta+6)x^3y^3 + (6\alpha\beta-4\alpha)x^3y^6]$$

$$= D_x^{\frac{1}{2}}[4x^3 + (2\beta+2)x^4 + (4\alpha-4)x^4 + (4\alpha+4\beta-8)x^5 + 4\alpha x^8]$$

$$+ D_x^{\frac{1}{2}}[(6\alpha\beta-6\alpha-6\beta+6)x^6 + (6\alpha\beta-4\alpha)x^9]$$

$$= 4\sqrt{3}x^3 + 2(2\beta+2)x^4 + 2(4\alpha-4)x^4 + \sqrt{5}(4\alpha+4\beta-8)x^5 + 4\sqrt{8}\alpha x^8 + \sqrt{6}(6\alpha\beta-6\alpha-6\beta+6)x^6 + 3(6\alpha\beta-4\alpha)x^9.$$

ii. $D_x^{\frac{1}{2}}JS_y^{\frac{1}{2}}S_x^{\frac{1}{2}}(M(G;x,y)) = D_x^{\frac{1}{2}}JS_y^{\frac{1}{2}}S_x^{\frac{1}{2}}[4xy^2 + (2\beta+2)xy^3 + (4\alpha-4)x^2y^2 + (4\alpha+4\beta-8)x^2y^3 + 4\alpha x^2y^6] + D_x^{\frac{1}{2}}JS_y^{\frac{1}{2}}S_x^{\frac{1}{2}}[(6\alpha\beta-6\alpha-6\beta+6)x^3y^3 + (6\alpha\beta-4\alpha)x^3y^6]$

$$= D_x^{\frac{1}{2}}JS_y^{\frac{1}{2}}\left[4xy^2 + (2\beta+2)xy^3 + \frac{1}{\sqrt{2}}(4\alpha-4)x^2y^2 + \frac{1}{\sqrt{2}}(4\alpha+4\beta-8)x^2y^3 + \frac{4}{\sqrt{2}}x^2y^6\right]$$

$$+ D_x^{\frac{1}{2}}JS_y^{\frac{1}{2}}\left[\frac{1}{\sqrt{3}}(6\alpha\beta-6\alpha-6\beta+6)x^3y^3 + (\frac{1}{\sqrt{3}}(6\alpha\beta-4\alpha)x^3y^6\right]$$

$$= D_x^{\frac{1}{2}}J\left[\frac{4}{\sqrt{2}}xy^2 + \frac{1}{\sqrt{3}}(2\beta+2)xy^3 + \frac{1}{2}(4\alpha-4)x^2y^2 + \frac{1}{\sqrt{6}}(4\alpha+4\beta-8)x^2y^3 + \frac{4}{\sqrt{12}}\alpha x^2y^6\right] + D_x^{\frac{1}{2}}J\left[\frac{1}{3}(6\alpha\beta-6\alpha-6\beta+6)x^3y^3 + \frac{1}{\sqrt{18}}(6\alpha\beta-4\alpha)x^3y^6\right]$$

$$= D_x^{\frac{1}{2}}\left[2\sqrt{2}x^3 + \frac{1}{\sqrt{3}}(2\beta+2)x^4 + \frac{1}{2}(4\alpha-4)x^4 + \frac{1}{\sqrt{6}}(4\alpha+4\beta-8)x^5 + \frac{2}{\sqrt{3}}\alpha x^8\right]$$

$$+D_x^{\frac{1}{2}}\left[\frac{1}{3}(6\alpha\beta-6\alpha-6\beta+6)x^6 + \frac{1}{\sqrt{18}}(6\alpha\beta-4\alpha)x^9\right]$$

$$= 2\sqrt{6}x^3 + 2\frac{1}{\sqrt{3}}(2\beta+2)x^4 + (4\alpha-4)x^4 + \frac{\sqrt{5}}{\sqrt{6}}(4\alpha+4\beta-8)x^5 + 4\frac{\sqrt{2}}{\sqrt{3}}\alpha x^8 + \frac{\sqrt{6}}{3}(6\alpha\beta-6\alpha-6\beta+6)x^6 + \frac{1}{\sqrt{2}}(6\alpha\beta-4\alpha)x^9.$$

iii. $S_x^{\frac{1}{2}}JD_y^{\frac{1}{2}}D_x^{\frac{1}{2}}(M(G;x,y)) = S_x^{\frac{1}{2}}JD_y^{\frac{1}{2}}D_x^{\frac{1}{2}}[4xy^2 + (2\beta+2)xy^3 + (4\alpha-4)x^2y^2 + (4\alpha+4\beta-8)x^2y^3]$

$$+S_x^{\frac{1}{2}}JD_y^{\frac{1}{2}}D_x^{\frac{1}{2}}[4\alpha x^2y^6+(6\alpha\beta-6\alpha-6\beta+6)x^3y^3+(6\alpha\beta-4\alpha)x^3y^6]$$

$$=S_x^{\frac{1}{2}}JD_y^{\frac{1}{2}}[4xy^2+(2\beta+2)xy^3+\sqrt{2}(4\alpha-4)x^2y^2+\sqrt{2}(4\alpha+4\beta-8)x^2y^3]$$

$$+S_x^{\frac{1}{2}}JD_y^{\frac{1}{2}}[4\sqrt{2}\alpha x^2y^6+\sqrt{3}(6\alpha\beta-6\alpha-6\beta+6)x^3y^3+\sqrt{3}(6\alpha\beta-4\alpha)x^3y^6]$$

$$=S_x^{\frac{1}{2}}J[4\sqrt{2}xy^2+\sqrt{3}(2\beta+2)xy^3+2(4\alpha-4)x^2y^2+\sqrt{6}(4\alpha+4\beta-8)x^2y^3]$$

$$+S_x^{\frac{1}{2}}J[4\sqrt{12}\alpha x^2y^6+3(6\alpha\beta-6\alpha-6\beta+6)x^3y^3+\sqrt{18}(6\alpha\beta-4\alpha)x^3y^6]$$

$$=S_x^{\frac{1}{2}}[4\sqrt{2}x^3+\sqrt{3}(2\beta+2)x^4+2(4\alpha-4)x^4+\sqrt{6}(4\alpha+4\beta-8)x^5+4\sqrt{12}\alpha x^8]$$

$$+S_x^{\frac{1}{2}}[3(6\alpha\beta-6\alpha-6\beta+6)x^6+\sqrt{18}(6\alpha\beta-4\alpha)x^9]$$

$$=4\frac{\sqrt{2}}{\sqrt{3}}x^3+\frac{\sqrt{3}}{2}(2\beta+2)x^4+(4\alpha-4)x^4+\frac{\sqrt{6}}{\sqrt{5}}(4\alpha+4\beta-8)x^5+4\frac{\sqrt{12}}{\sqrt{8}}\alpha x^8+\frac{3}{\sqrt{6}}(6\alpha\beta-6\alpha-6\beta+6)x^6+\frac{\sqrt{18}}{3}(6\alpha\beta-4\alpha)x^9.$$

Hence, the Nirmala indices of G are given by

$$(a)N(G)=D_x^{\frac{1}{2}}J(M(G;x,y))|_{x=1}$$
$$=(6\sqrt{6}+18)\alpha\beta+\left(4\sqrt{5}+4\sqrt{8}-6\sqrt{6}-4\right)\alpha+\left(4+4\sqrt{5}-6\sqrt{6}\right)\beta+4\sqrt{3}-4-8\sqrt{5}+6\sqrt{6}.$$

$$(b)IN_1(G)=D_x^{\frac{1}{2}}JS_y^{\frac{1}{2}}S_x^{\frac{1}{2}}(M(G;x,y))|_{x=1}$$
$$=(2\sqrt{6}+3\sqrt{2})\alpha\beta+\left(4+4\frac{\sqrt{5}}{\sqrt{6}}+4\frac{\sqrt{2}}{\sqrt{3}}-2\sqrt{6}-2\sqrt{2}\right)\alpha+\left(\frac{4}{\sqrt{3}}+4\frac{\sqrt{5}}{\sqrt{6}}-2\sqrt{6}\right)\beta+4\sqrt{6}+\frac{4}{\sqrt{3}}-4-8\frac{\sqrt{5}}{\sqrt{6}}.$$

$$(c)IN_2(G)=S_x^{\frac{1}{2}}JD_y^{\frac{1}{2}}D_x^{\frac{1}{2}}(M(G;x,y))|_{x=1}$$
$$=\left(3\sqrt{6}+6\sqrt{2}\right)\alpha\beta+\left(4+4\frac{\sqrt{6}}{\sqrt{5}}+4\frac{\sqrt{3}}{\sqrt{2}}-3\sqrt{6}-4\sqrt{2}-3\sqrt{6}\right)\alpha+\left(\sqrt{3}+4\frac{\sqrt{6}}{\sqrt{5}}-3\sqrt{6}\right)\beta+4\frac{\sqrt{2}}{\sqrt{3}}+\sqrt{3}-4-8\frac{\sqrt{6}}{\sqrt{5}}+3\sqrt{6}.$$

2.2. Entropy measures of TiO_2.

We proceed with the computation of graph entropy metrics for the titanium dioxide TiO_2. Initially, we assess the degree-based graph entropy expression. Subsequently, we determine the mathematical formulations for entropy measures based on Nirmala indices using the previously derived expressions of the Nirmala indices.

Degree-based entropy of TiO_2:

From Equation (7) and Table 2, we have

$$ENT_{\omega}(G) = log(2q) - \frac{1}{2q}\sum_{i=1}^{p} d_G(s_i)log(d_G(s_i))$$

$$= log(2(12\alpha\beta + 2\alpha)) - \frac{1}{2(12\alpha\beta+2\alpha)} \times \left[\sum_{s\in V_1(G)} d_G(s)log\left(d_G(s)\right) + \sum_{s\in V_2(G)} d_G(s)log(d_G(s)) + \sum_{s\in V_3(G)} d_G(s)log(d_G(s))\right]$$

$$= log(2(12\alpha\beta + 2\alpha)) - \frac{1}{2(12\alpha\beta+2\alpha)}$$

$$\times [1 \cdot (2\beta + 6) \cdot log(1) + 2 \cdot (8\alpha + 2\beta - 6) \cdot log(2)]$$

$$+[3 \cdot (6\alpha\beta - 4\alpha - 2\beta + 2) \cdot log(3) + 6 \cdot \alpha\beta \cdot log(6)]$$

$$= log(24\alpha\beta + 4\alpha) - log(2)\frac{16\alpha + 4\beta - 12}{24\alpha\beta + 4\alpha} + log(3)\frac{18\alpha\beta - 12\alpha - 6\beta + 6}{24\alpha\beta + 4\alpha}$$

$$+ log(6)\frac{6\alpha\beta}{24\alpha\beta + 4\alpha}.$$

Nirmala entropy of TiO_2: From Theorem 2, the Nirmala index of G is given by:

$$N(G) = (6\sqrt{6} + 18)\alpha\beta + \left(4\sqrt{5} + 4\sqrt{8} - 6\sqrt{6} - 4\right)\alpha + \left(4 + 4\sqrt{5} - 6\sqrt{6}\right)\beta + 4\sqrt{3} - 4 - 8\sqrt{5} + 6\sqrt{6}.$$

From Table 3 and Equation (8), we have

$$ENT_N(G) = log(N(G)) - \frac{1}{N(G)}\sum_{st\in E(G)} \sqrt{d_G(s) + d_G(t)} \times log(\sqrt{d_G(s) + d_G(t)})$$

$$= log(N(G)) - \frac{1}{N(G)}\left[\sum_{i=1}^{4}\sum_{st\in E_i(G)} \sqrt{d_G(s) + d_G(t)} \times log(\sqrt{d_G(s) + d_G(t)})\right]$$

$$= log(N(G)) - \frac{1}{N(G)}([4\sqrt{3} \cdot log(\sqrt{3}) + 32(\beta + 1)(\alpha - 1) \cdot log(2) + 4\sqrt{5} \cdot (\alpha + \beta - 2) \cdot log(\sqrt{5})] \quad - \frac{1}{N(G)}\left[4\sqrt{8}\alpha \cdot log(\sqrt{8}) + 6\sqrt{6}(\alpha\beta - \alpha - \beta + 1) \cdot log(\sqrt{6}) + 6(3\alpha\beta - 2\alpha) \cdot log(3)\right]$$

Finally, we get the desired formulation of the Nirmala entropy for TiO_2 by substituting the value of $N(G)$ into the previous expression.

First inverse Nirmala entropy of TiO_2: From Theorem 2, the first inverse Nirmala index G is given by

$$IN_1(G) = (2\sqrt{6} + 3\sqrt{2})\alpha\beta + \left(4 + 4\frac{\sqrt{5}}{\sqrt{6}} + 4\frac{\sqrt{2}}{\sqrt{3}} - 2\sqrt{6} - 2\sqrt{2}\right)\alpha + \left(\frac{4}{\sqrt{3}} + 4\frac{\sqrt{5}}{\sqrt{6}} - 2\sqrt{6}\right)\beta$$
$$+4\sqrt{6} + \frac{4}{\sqrt{3}} - 4 - 8\frac{\sqrt{5}}{\sqrt{6}}.$$

From Table 3 and Equation (9), we have

$$ENT_{IN_1}(G) = log(IN_1(G)) - \frac{1}{IN_1(G)}\sum_{st\in E(G)} \sqrt{\frac{1}{d_G(s)} + \frac{1}{d_G(t)}} \times log\left(\sqrt{\frac{1}{d_G(s)} + \frac{1}{d_G(t)}}\right)$$

$$= log(IN_1(G)) - \frac{1}{IN_1(G)}\left[\sum_{i=1}^{4}\sum_{st\in E_i(G)} \sqrt{\frac{1}{d_G(s)} + \frac{1}{d_G(t)}} \times log\left(\sqrt{\frac{1}{d_G(s)} + \frac{1}{d_G(t)}}\right)\right]$$

$$= log(IN_1(G)) - \frac{1}{IN_1(G)}\left[4\frac{\sqrt{3}}{\sqrt{2}}\cdot log(\frac{\sqrt{3}}{\sqrt{2}}) + \frac{4}{\sqrt{3}}(\beta+1)\cdot log(\frac{2}{\sqrt{3}}) + \frac{\sqrt{5}}{\sqrt{6}}(4\alpha+4\beta-8)\cdot log\frac{\sqrt{5}}{\sqrt{6}}\right]$$
$$- \frac{1}{IN_1(G)}\left[4\frac{\sqrt{2}}{\sqrt{3}}\alpha\cdot log(\frac{\sqrt{2}}{\sqrt{3}}) + \frac{\sqrt{2}}{\sqrt{3}}(6\alpha\beta-6\alpha-6\beta+6)\cdot log(\frac{\sqrt{2}}{\sqrt{3}}) + \frac{1}{\sqrt{2}}(6\alpha\beta-4\alpha)\cdot log\left(\frac{1}{\sqrt{2}}\right)\right].$$

Finally, by substituting the value of $IN_1(G)$ into the preceding expression, we obtain the desired formulation of the first inverse Nirmala entropy for TiO_2.

Second inverse Nirmala entropy of TiO_2: From Theorem 2, the second inverse Nirmala index G is given by

$$IN_2(\Upsilon) = (3\sqrt{6}+6\sqrt{2})\alpha\beta + (4+4\frac{\sqrt{6}}{\sqrt{5}}+4\frac{\sqrt{3}}{\sqrt{2}}-3\sqrt{6}-4\sqrt{2}-3\sqrt{6})\alpha + \left(\sqrt{3}+4\frac{\sqrt{6}}{\sqrt{5}}-3\sqrt{6}\right)\beta + 4\frac{\sqrt{2}}{\sqrt{3}}-\sqrt{3}-4-8\frac{\sqrt{6}}{\sqrt{5}}+3\sqrt{6}.$$

From Table 3 and Equation (10), we have

$$ENT_{IN_2}(G) = log(IN_2(G)) - \frac{1}{IN_2(G)}\sum_{st\in E(G)}\frac{\sqrt{d_G(s)\cdot d_G(t)}}{\sqrt{d_G(s)+d_G(t)}}\times log\left(\frac{\sqrt{d_G(s)\cdot d_G(t)}}{\sqrt{d_G(s)+d_G(t)}}\right)$$
$$= log(IN_2(G)) - \frac{1}{IN_2(G)}\left[\sum_{i=1}^{4}\sum_{st\in E_i(G)}\frac{\sqrt{d_G(s)\cdot d_G(t)}}{\sqrt{d_G(s)+d_G(t)}}\times log\left(\frac{\sqrt{d_G(s)\cdot d_G(t)}}{\sqrt{d_G(s)+d_G(t)}}\right)\right]$$
$$= log(IN_2(G)) - \frac{1}{IN_2(G)}\left[4\frac{\sqrt{2}}{\sqrt{3}}\cdot log(\frac{\sqrt{2}}{\sqrt{3}}) + \left(\sqrt{3}(\beta+1)\cdot log(\frac{\sqrt{3}}{2}\right)\right]$$
$$- \frac{1}{IN_2(G)}\left[\frac{\sqrt{6}}{\sqrt{5}}(4\alpha+4\beta-8)\cdot log(\frac{\sqrt{6}}{\sqrt{5}}) + 4\frac{\sqrt{3}}{\sqrt{2}}\alpha\cdot log(\frac{\sqrt{3}}{\sqrt{2}})\right]$$
$$- \frac{1}{IN_2(G)}\left[\frac{\sqrt{3}}{\sqrt{2}}(6\alpha\beta-6\alpha-6\beta+6)\cdot log(\frac{\sqrt{3}}{\sqrt{2}}) + \sqrt{2}(6\alpha\beta-4\alpha)\cdot log(\sqrt{2})\right].$$

The second inverse Nirmala entropy for TiO_2 can finally be expressed as desired by changing the value of $IN_2(G)$ in the previous expression.

3. Comparison Through Numerical and Graphical Demonstrations

Many scientific fields, such as computer science, information theory, chemistry, biological medicine, and pharmacology, extensively use graph entropy metrics. As such, to properly describe these molecular descriptors, scientists working in these domains rely on numerical computation and graphical representation. This section uses 2D line graphs and numerical computation to compare the Nirmala indices and the accompanying entropy measures.

Table 4 shows the results of the numerical computation of the Nirmala indices and corresponding entropy measures for TiO_2, where $1 \le \alpha \le 25$ and $1 \le \beta \le 25$, provided that $\alpha = \beta$. Furthermore, Figure 1 compares the Nirmala indices and relevant entropy measures using 2D line plots for $2 \le \alpha, \beta \le 25$ with $\alpha = \beta$.

Table 4. Results of the numerical calculation of the Nirmala indices and corresponding entropy measures for the titanium dioxide TiO_2, where $1 \leq \alpha \leq 25, 1 \leq \beta \leq 25$ with $\alpha = \beta$.

$[\alpha, \beta]$	N	IN_1	IN_2	ENT_N	ENT_{IN_1}	ENT_{IN_2}
[1,1]	32.2419	14.1979	7.1090	2.6139	2.6175	1.8469
[2,2]	130.14	45.874	46.302	3.9350	3.9330	3.6039
[3,3]	293.43	95.8348	117.163	4.7234	4.7218	4.5121
[4,4]	522.12	164.078	219.692	5.2874	5.2864	5.1324
[5,5]	816.20	250.604	353.888	5.7267	5.7263	5.60
[6,6]	1175.67	355.414	519.75	6.0867	6.0867	5.9861
[7,7]	1600.54	478.507	717.28	6.3917	6.3920	6.3062
[8,8]	2090.8	619.883	946.48	6.6563	6.6568	6.5821
[9,9]	2646.4	779.543	1207.34	6.8899	6.8906	6.8244
[10,10]	3267.5	957.486	1499.88	7.0991	7.0999	7.0405
[11,11]	3953.9	1153.71	1824.08	7.2884	7.2894	7.2355
[12,12]	4705.7	1368.22	2179.95	7.4614	7.4625	7.4131
[13,13]	5523.02	1601.01	2567.48	7.6205	7.6218	7.5763
[14,14]	6405.6	1852.08	2986.69	7.7680	7.7693	7.7271
[15,15]	7353.6	2121.44	3437.56	7.9053	7.9067	7.8674
[16,16]	8367.08	2409.09	3920.10	8.0338	8.0352	7.9984
[17,17]	9445.89	2715.01	4434.30	8.1545	8.1560	8.1214
[18,18]	10590	3039.22	4980.18	8.2684	8.2699	8.2373
[19,19]	11799	3381.71	5557.72	8.3761	8.3777	8.3468
[20,20]	13074	3742.49	6166.92	8.4783	8.4800	8.4506
[21,21]	14415	4121.55	6807.80	8.5755	8.5772	8.5493
[22,22]	15820	4518.89	7480.34	8.6683	8.6700	8.6433
[23,23]	17292	4934.51	8184.56	8.7569	8.7587	8.7332
[24,24]	18828	5368.42	8920.43	8.8418	8.8436	8.8191
[25,25]	20430	5820.6	9687.9	8.9232	8.9250	8.9016

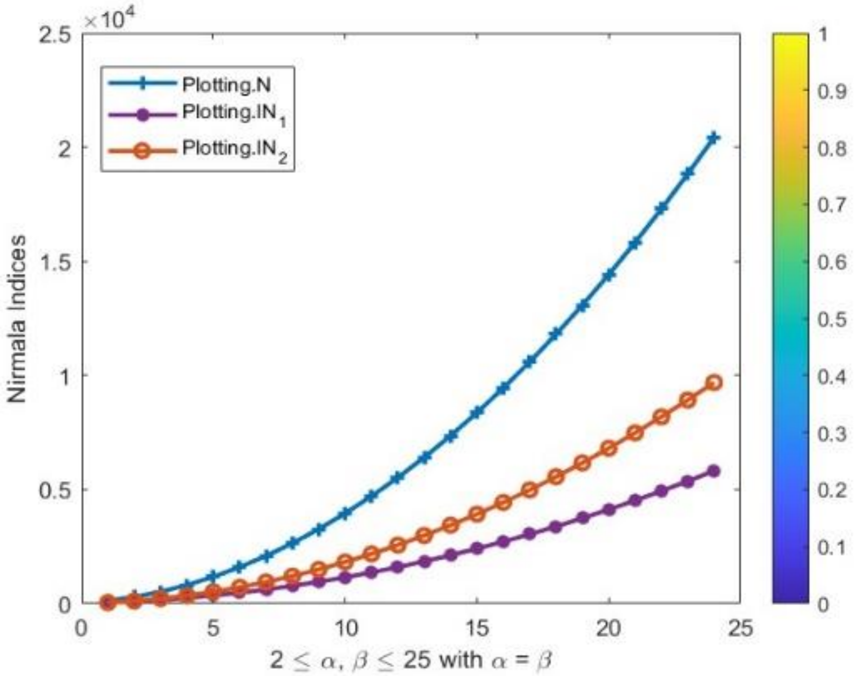

(a)

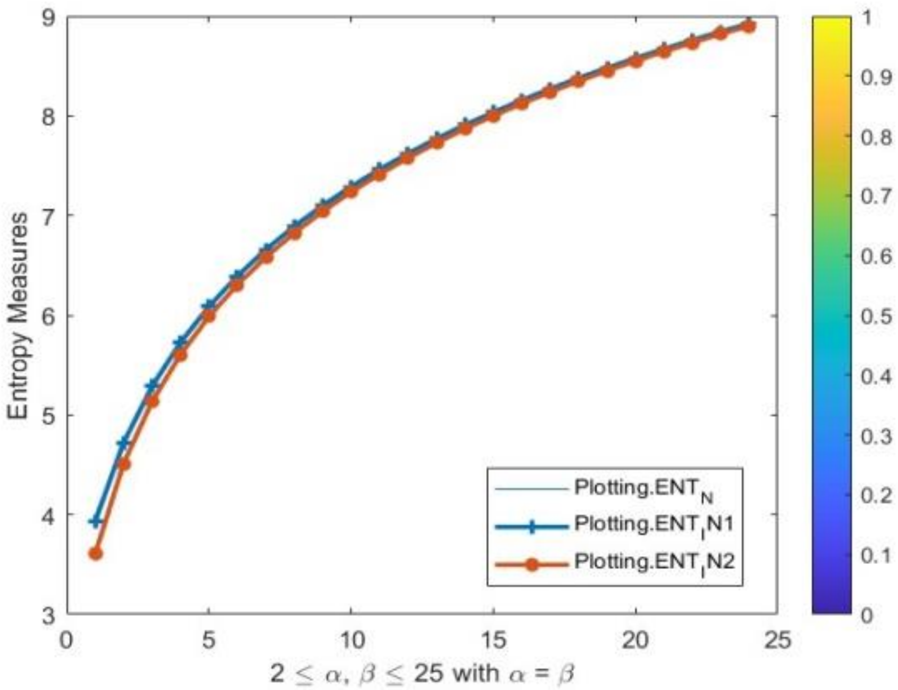

(b)

Figure 1. Comparison of the Nirmala indices (a) and their associated entropy measures (b) of TiO_2 through a 2D line plot for $2 \leq \alpha \leq 25, 2 \leq \beta \leq 25$ with $\alpha = \beta$.

The following are the observations from Table 4 and Figure 1.

Observation 1: The entropy values increase with the dimension of the titanium dioxide TiO_2, which confirms that they are directly proportional to each other.

Observation 2: For the molecular graph G of titanium dioxide TiO_2, the following inequality relationships are possible:

(i) $IN_2(G) < IN_1(G) < N(G)$ for $\alpha = \beta = 1$; $IN_1(G) < IN_2(G) < N(G)$ for $2 \leq \alpha \leq 25, 2 \leq \beta \leq 25$ with $\alpha = \beta$.

(ii) $ENT_{IN_2}(G) < ENT_{IN_1}(G)$; $ENT_{IN_2}(G) < ENT_N(G)$ for $1 \leq \alpha \leq 25, 1 \leq \beta \leq 25$ with $\alpha = \beta$.

(iii) $ENT_N(G) \approx ENT_{IN_1}(G)$ for $1 \leq \alpha \leq 25, 1 \leq \beta \leq 25$ with $\alpha = \beta$.

4. The Logarithmic Regression Model

To investigate the relationship between the dependent variable and one or more predictor variables in our dataset, we used logarithmic regression analysis. This nonlinear regression technique modifies the dependent or predictor variables using logarithmic functions.

A logarithmic regression model has the following equation: $y = a * log(x) + b$, where x is the predictor variable, and y is the response variable. The regression coefficients a and b represent the relationship between x and y. In this analysis, we perform logarithmic regression to investigate the relationship between the Nirmala indices and entropy measures of titanium dioxide for $1 \leq \alpha, \beta \leq 25$ with $\alpha = \beta$. The statistical measures used in this investigation include the squared correlation coefficient (R^2), the sum of squared errors (SSE), the adjusted squared correlation coefficient (Adj. R-sq), and the root mean square error (RMSE). A low RMSE value (closer to 0) indicates efficient model performance, while a high R^2 value (closer to 1) suggests that the regression line fits the data well. Our primary objective in this situation is to achieve a higher R^2 value.

The statistics for the curve fitting of the Nirmala indices versus Nirmala entropy measures for titanium dioxide, using logarithmic regression, are presented in Table 5.

Table 5. Statistics of curve fitting of the Nirmala indices vs. Nirmala of titanium dioxide.

Model	R^2	SSE	Adj. R-sq	RMSE
$ENT_N = 0.9837 * log(N) - 0.8523$	**0.9999**	0.0004636	0.9999	0.0141
$ENT_{IN_1} = 1.0358 * log(IN_1) - 0.0282$	**0.9997**	0.0195	0.9996	0.02918
$ENT_{IN_2} = 0.9853 * log(IN_2) - 0.1569$	**0.9998**	0.0090	0.9998	0.0197

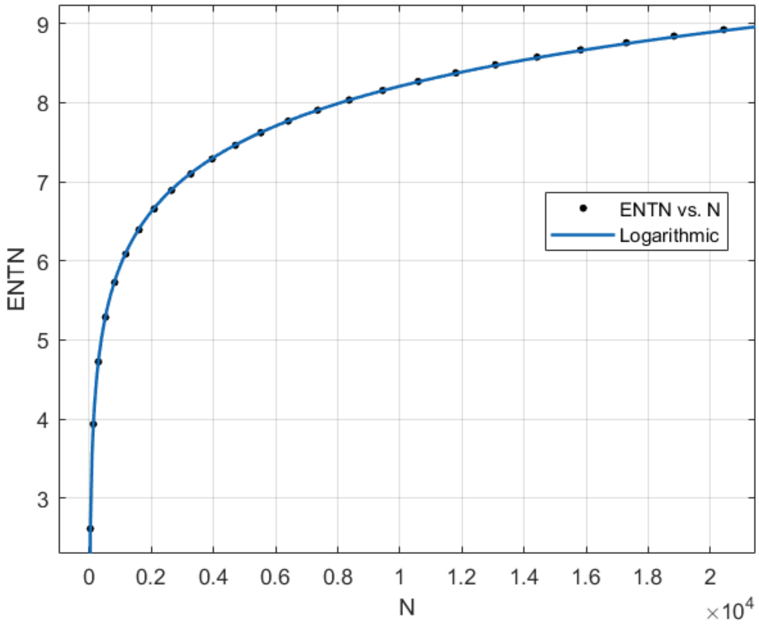

(a)

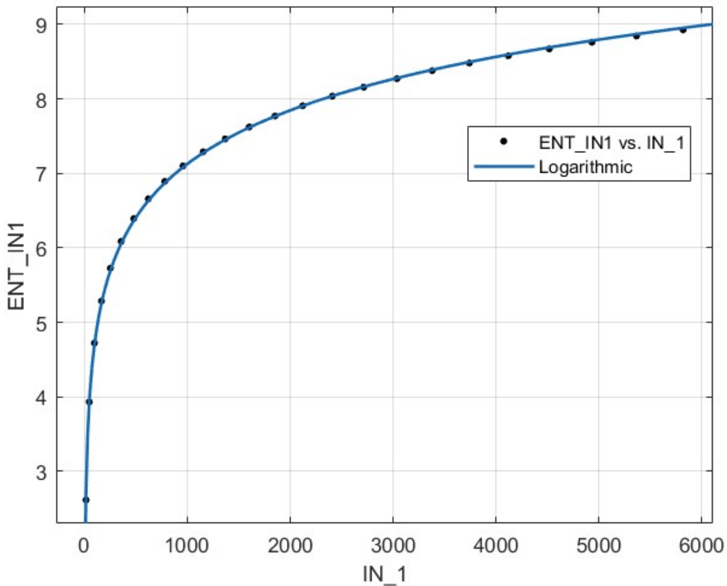

(b)

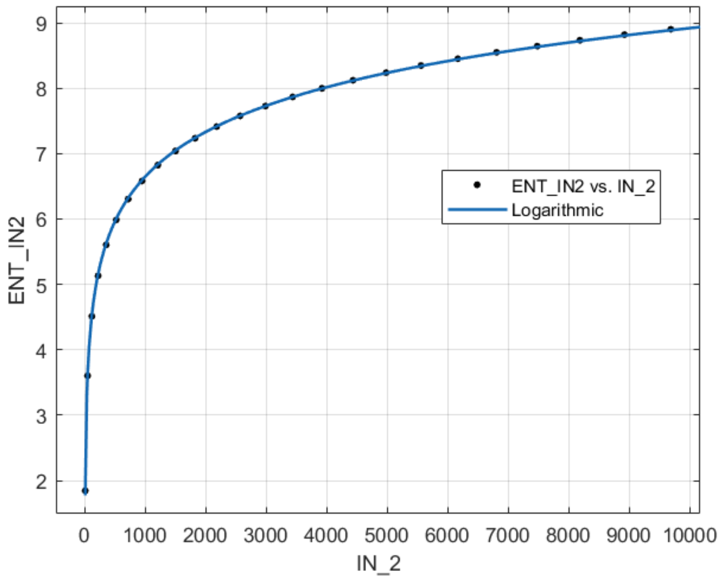

(c)

Figure 2. Curve fitting plots for: (a) Nirmala index and its corresponding entropy measure, (b) First inverse Nirmala index and its corresponding entropy measure, (c) Second inverse Nirmala index and its corresponding entropy measure of TiO_2.

5. Discussion

Topological indices, which quantify molecular structures, help in studying molecular properties and the behavior of chemical and biological systems. Accurate calculation of these numerical indices provides researchers with valuable insights into the systems under investigation. In this work, we study the so-called Nirmala indices, which are degree-based topological indices of titanium dioxide. The Nirmala indices and corresponding entropy measures of titanium dioxide increase as α and β increase, according to Table 4 and Figure 1.

Entropy measures quantify the uncertainty in a dataset and help determine its complexity and distribution. They are widely used in fields such as information theory, thermodynamics, and data analysis. Accurate computations of numerical entropy provide researchers with essential information that enhances their comprehension of the network under study. This validates our attention on the vertex and edge weight entropy of TiO_2. Table 4 and Figure 1 show that the entropy measures of the titanium dioxide TiO_2 increase as α and β increase. The social sciences, biology, and economics all use logarithmic regression, a type of non-linear regression, to make predictions and account for data that doesn't follow a straight line. Table 5 shows the statistical parameters, such as the squared correlation coefficient (R^2), the sum of square errors (SSE), and the root mean square errors (RMSE). If R^2 is higher (nearer to 1), it means that the regression line fits the data better.

From Figure 2, we can see that the Nirmala indices and the corresponding entropy measure values for TiO_2 also look good and fit the curve.

6. Conclusion

The definitions of the Nirmala indices and the entropy measures based on them have been used in this research work. The Nirmala indices of the titanium dioxide TiO_2 have been mathematically formulated. Its M-polynomial has been used to analyze the Nirmala indices-based entropy measures. Additionally, the Nirmala indices and related entropy measures have been numerically computed and shown in a 2D line plot, and we have compared them using

2D line plots. The Nirmala indices and associated entropy measures of titanium dioxide TiO_2 increase as the values of α and β increase, according to Table 4 and Figure 1.

For the molecular graph G of the titanium dioxide, we have the following inequality relationships:

(i) $IN_2(G) < IN_1(G) < N(G)$ for $\alpha = \beta = 1$; $IN_1(G) < IN_2(G) < N(G)$ for $2 \leq \alpha \leq 25, 2 \leq \beta \leq 25$ with $\alpha = \beta$.

(ii) $ENT_{IN_2}(G) < ENT_{IN_1}(G)$; $ENT_{IN_2}(G) < ENT_N(G)$ for $1 \leq \alpha \leq 25, 1 \leq \beta \leq 25$ with $\alpha = \beta$.

(iii) $ENT_N(G) \approx ENT_{IN_1}(G)$ for $1 \leq \alpha \leq 25, 1 \leq \beta \leq 25$ with $\alpha = \beta$.

Although some research claims that TiO_2 nanoparticles cause no harm to people by consumption or skin contact, strong data show their toxicity in animal models. . Moreover, for the thorough characterization of TiO_2 nanoparticles in food and cosmetic items, international authorities do not have any formal, consistent policies. These discoveries could depend critically on the future use of TiO_2 as a food additive or sunscreen component. These findings may provide valuable insights for future advancements in the use of TiO_2 as a food additive or sunscreen compound.

Funding

There is no funding.

Acknowledgments

Declared none.

Conflicts of Interest

The authors declare no conflict of interest.

References

1. Kelly, T.D.; Matos, G.R. Titanium dioxide end-use statistics, 1975-2004. Historical Statistics for Mineral and Material Commodities in the United States; Data Series 140; U.S. Geological Survey: Reston, VA, USA, **2005**; https://doi.org/10.3133/ds140.
2. Piccinno, F.; Gottschalk, F.; Seeger, S.; Nowack, B. Industrial production quantities and uses of ten engineered nanomaterials in Europe and the world. *J. Nanopart. Res*. **2012**, *14*, 1109, https://doi.org/10.1007/s11051-012-1109-9.
3. Weir, A.; Westerhoff, P.; Fabricius, L.; N. von Goetz. Titanium dioxide nanoparticles in food and personal care products. *Environ. Sci. Technol*. **2012**, *46*, 2242-2250, https://doi.org/10.1021/es204168d.
4. Ziental, D.; Czarczynska-Goslinska, B.; Mlynarczyk, D.T.; Glowacka-Sobotta, A.; Stanisz, B.; Goslinski, T.; Sobotta, L. Titanium dioxide nanoparticles: Prospects and applications in medicine. *Nanomaterials* **2020**, *10*, 387, https://doi.org/10.3390/nano10020387.
5. Wang, Q.; Huang, J.Y.; Li, H.; Chen, Z.; Zhao, Z.A.Z.; Wang, Y.; Zhang, K.; Sun, H.T.; Al-Deyab, S.S.; Lai, Y.K. TiO_2 nanotube platforms for smart drug delivery: A review. *Int. J. Nanomed*. **2016**, *11*, 4819-4834, https://doi.org/10.2147/IJN.S108847.
6. Babitha, S.; Korrapati, P.S. Biodegradable zein-polydopamine polymeric scaffold impregnated with TiO_2 nanoparticles for skin tissue engineering. *Biomed. Mater*. **2017**, *12*, 055008, https://doi.org/10.1088/1748605X/aa7d5a.
7. Stan, M.S.; Nica, I.C.; Dinischiotu, A.; Varzaru, E.; Iordache, O.G.; Dumitrescu, I.; Popa, M.; Chifiriuc, M.C.; Pircalabioru, G.G.; Lazar, V. Photocatalytic, antimicrobial and biocompatibility features of cotton knit coated with Fe-N-Doped titanium dioxide nanoparticles. *Materials* **2016**, *9*, 789, https://doi.org/10.3390/ma9090789.

8. Seisenbaeva, G.A.; Fromell, K.; Vinogradov, V.V.; Terekhov, A.N.; Pakhomov, A.V.; Nilsson, B.; Ekdahl, K.N.; Vinogradov, V.V.; Kessler, V.G. Dispersion of TiO_2 nanoparticles improves burn wound healing and tissue regeneration through specific interaction with blood serum proteins. *Sci. Rep*. **2017**, *7*, 15448, https://doi.org/10.1038/s41598-017-15792-w.
9. Deng, D.; Kim, M.G.; Lee, J.Y.; Cho, J. Green energy storage materials: Nanostructured TiO_2 and Sn-based anodes for lithium-ion batteries. *Energy Envron. Sci*. **2009**, *2*, 818-837, https://doi.org/10.1039/B823474D.
10. Sharma, S.; Sharma, R.K.; Gaur, K.; CÃtala Torres, J.F.; Loza-Rosas, S.A.; Torres, A.; Saxena, M.; Julin, M.; Tinoco, A.D. Fueling a hot debate on the application of TiO_2 nanoparticles in sunscreen. *Materials* **2019**, *12*, 2317, https://doi.org/10.3390/ma12142317.
11. Liang, C.; Zhang, X.; Fang, J.; Sun, N.; Liu, H.; Feng, Y.; Wang, H.; Yu.Z.; Jia, X. Genotoxicity evaluation of food additive titanium dioxide using a battery of standard in vivo tests. *Regulatory Toxicology and Pharmacology* **2024**, *148*, 105586, https://doi.org/10.1016/j.yrtph.2024.105586.
12. Musial, J.; Krakowiak, R.; Mlynarczyk, D.T.; Goslinski, T.; Stanisz, B.J. Titanium Dioxide Nanoparticles in Food and Personal Care Products - What Do We Know about Their Safety?. *Nanomaterials* **2020**, *10*, 1110, https://doi.org/10.3390/nano10061110.
13. Siddiqui, M.K.; Sana Javed, Khalid, S.; Amin.N.; Hussain, M. On network construction and module detection for the molecular graph of titanium dioxide. *Journal of Biomolecular Structure and Dynamics* **2023**, *41*, 10591-10603, https://doi.org/10.1080/07391102.2022.2155703.
14. Latha, T.S.; Reddy, M.C.; Durbaka, P.V.; Muthukonda. S.V.; Lomada, D. Immunomodulatory properties of titanium dioxide nanostructural materials. *Indian Journal of Pharmacology* **2017**, *49*, 458-464, https://doi.org/10.4103/ijp.IJP_536_16.
15. Zhu, X.; He, M.; Sun, Y.; Xu, Z.; Wan, Z.; Hou, D.; Alessi, D.S.; Tsang, D.C.W. Insights into the adsorption of pharmaceuticals and personal care products (PPCPs) on biochar and activated carbon with the aid of machine learning. *Journal of Hazardous Materials* **2022**, *423*, 127060-127017, https://doi.org/10.1016/j.jhazmat.2021.127060.
16. Du, N.; Chen, M.; Cui, Y.; Liu, X.; Li, Y. Fluorescent sensor array constructed by functionalized carbon nanodots for qualitative and quantitative analysis of urinary organic acid biomarkers. *Sensors and Actuators B: Chemical* **2022**, *350*, 130825-130819, https://doi.org/10.1016/j.snb.2021.130825.
17. Xiao, Y.; Li, H.; Liu, Y.; Chen, C.; Cang, H.; Li, M.; Xu, Y.; Yang, Q.; Wang, X.; Li, H. Pulse purge thermal desorption ion mobility spectrometer for rapid and sensitive determination of intravenous anesthetic etomidate in blood. *Sensors and Actuators B: Chemical* **2022**, *350*, 130844-130814, https://doi.org/10.1016/j.snb.2021.130844.
18. Langfelder, P.; Horvath, S. WGCNA: An R package for weighted correlation network analysis. *BMC Bioinformatics* **2008**, *9*, 559-566, https://doi.org/10.1186/1471-2105-9-559.
19. Zhang, D.; Zong, X.; Wu, Z.; Zhang, Y. Ultrahigh-performance impedance humidity sensor based on layer-by-layer self-assembled tin disulfide/titanium dioxide nanohybrid film. *Sensors and Actuators B: Chemical* **2018**, *266*, 52-62, https://doi.org/10.1016/j.snb.2018.03.007.
20. Pan, W.; Zhang, Y.; Zhang, D. Self-assembly fabrication of titanium dioxide nanospheres-decorated tungsten diselenide hexagonal nanosheets for ethanol gas sensing application. *Applied Surface Science* **2020**, *527*, 46781-146712, https://doi.org/10.1016/j.apsusc.2020.146781.
21. Wu, J.; Zhang. D.; Cao, Y. Fabrication of iron-doped titanium dioxide quantum dots/molybdenum disulfide nanoflower for ethanol gas sensing. *Journal of Colloid and Interface Science* **2018**, *529*, 556-567, https://doi.org/10.1016/j.jcis.2018.06.049.
22. Shukla, R.K.; Kumar, A.; Gurbani, D.; Pandey, A.K.; Singh, S.; Dhawan, A. TiO_2 nanoparticles induce oxidative DNA damage and apoptosis in human liver cells. *Nanotoxicology* **2013**, *7*, 48-60, https://doi.org/10.3109/17435390.2011.629747.
23. Zhang, H.; Banfield, J.F. Structural characteristics and mechanical and thermodynamic properties of nanocrystalline TiO_2 C*hemical Reviews* **2014**, *114*, 9613-9644, https://doi.org/10.1021/cr500072j.
24. Hu, Y.; Tsai, H.L.; Huang, C.L. Effect of brookite phase on the anatase-rutile transition in titania nanoparticles. *Journal of the European Ceramic Society* **2003**, *23*, 691-696, https://doi.org/10.1016/S0955-2219(02)00194-2.
25. Che, X.; Li, L.; Zheng, J.; Li, G.; Shi, Q. Heat capacity and thermodynamic functions of brookite TiO_2. *The Journal of Chemical Thermodynamics* **2016**, *93*, 45-51, https://doi.org/10.1016/j.jct.2015.09.018.

26. Blanchart, P. Extraction, Properties and Applications of Titania. In Industrial Chemistry of Oxides for Emerging Applications; Pawłowski, L., Blanchart, P., Eds.; John Wiley & Sons: **2018**; pp. 255-309, https://doi.org/10.1002/9781119424079.ch6.
27. Deng, H.; Yang, J.; Xia, F. A general modeling of some vertex-degree based topological indices in benzenoid systems and phenylenes. *Comput. Math. with Appl*. **2011**, *61*, 3017-3023, https://doi.org/10.1016/j.camwa.2011.03.089.
28. Wiener, H. Structural determination of paraffin boiling points. *J. Am. Chem. Soc*. **1947**, *69*, 17-20, https://doi.org/10.1021/ja01193a005.
29. Randić, M. Characterization of molecular branching. *J. Am. Chem. Soc*. **1975**, *97*, 6609-6615, https://doi.org/10.1021/ja00856a001.
30. Kulli, V.R. Nirmala index. *Int. J. Math. Trends Technol*. **2021**, 67, 8-12, https://doi.org/10.14445/22315373/IJMTT-V67I3P502.
31. Kulli, V.R.; Lokesha, V.; Nirupadi, K. Computation of inverse Nirmala indices of certain nanostructures. *International J. Math. Combin*. **2021**, *2*, 33-40.
32. Verma, A.; Mondal, S.; De, N.; Pal, A. Topological properties of bismuth tri-iodide using neighborhood M-polynomial. *Int. J. Math. Trends Technol*. **2019**, *67*, 83-90, https://doi.org/10.14445/22315373/IJMTT-V65I10P512.
33. Hosoya, H. On some counting polynomials in Chemistry. *Discrete Appl. Math*. **1988**, *19*, 239-257, https://doi.org/10.1016/0166-218X(88)90017-0.
34. Deutsch, E.; Klavžar, S. M-polynomial and degree-based topological indices. *Iran. J. Math. Chem*. **2015**, *6*, 93-102, https://doi.org/10.22052/IJMC.2015.10106.
35. Shannon, C.E. A mathematical theory of communication. *Bell Syst. Tech. J*. **1948**, *27*, 379-423, https://doi.org/10.1002/j.1538-7305.1948.tb01338.x.
36. Wang, X.L.; Siddiqui, M.K.; Kirmani, S.A.; Manzoor, S.; Ahmad, S.; Dhlamini, M. On topological analysis of entropy measures for silicon carbides networks. *Complexity* **2021**, *2021*, 1-26, https://doi.org/10.1155/2021/4178503.
37. Manzoor, S.; Siddiqui, M.K.; Ahmad, S. On entropy measures of polycyclic hydroxy-chloroquine used for novel coronavirus (COVID-19) treatment. *Polycycl. Aromat. Compd*. **2022**, *42*, 2947-2969, https://doi.org/10.1080/10406638.2020.1852289.
38. Manzoor, S.; Siddiqui, M.K.; Ahmad, S. On entropy measures of molecular graphs using topological indices. *Arab. J. Chem*. **2020**, *13*, 6285-6298, https://doi.org/10.1016/j.arabjc.2020.05.021.
39. Chen, Z.; Dehmer, M.; Shi, Y. A note on distance-based graph entropies. *Entropy* **2014**, *16*, 5416-5427, https://doi.org/10.3390/e16105416.
40. Kumar, V.; Das, S. On Nirmala Indices-based Entropy Measures of Silicon Carbide Network. *Iran. J. Math. Chem*. **2023**, *14*, 271-288, https://doi.org/10.22052/IJMC.2023.252742.1704.